Iranian Journal of
Numerical Analysis and Optimization

Ferdowsi University of Mashhad

Reaserch Article

Behavioral modeling and control strategies for Rumor-induced customer dynamics on digital platforms

S. Belhdid, H. Hassouni, O. Aarabate and O. Balatif

DOI:10.22067/ijnao.2026.96859.1794

Vol. 17, No. 1, March 2027

pp. 72–108

Ferdowsi University of Mashhad, Iran

Iranian Journal of Numerical Analysis and Optimization
Vol. 17, No. 1, 2027, pp 72–108
https://doi.org/10.22067/ijnao.2026.96859.1794
https://ijnao.um.ac.ir/

CC BY NC

Research Article

Behavioral modeling and control strategies for Rumor-induced customer dynamics on digital platforms

S. Belhdid*, H. Hassouni, O. Aarabate and O. Balatif

Abstract

This paper proposes a compartmental mathematical model for analyzing rumor-induced behavioral dynamics among customers on digital platforms. The customer population is divided into three the model captures how misinformation influences transitions between these states. The positivity and boundedness of the solutions are established, and the basic reproduction

*Corresponding author

Received 5 December 2025; revised 13 May 2026; accepted 5 August 2026

Salaheddine Belhdid
Laboratory of Fundamental Mathematics and their Applications, Department of Mathematics, Faculty of Sciences El Jadida, Chouaib Doukkali University, El Jadida, Morocco. e-mail: salaheddine.belhdid@gmail.com

Habib Hassouni
Laboratory of Fundamental Mathematics and their Applications, Department of Mathematics, Faculty of Sciences El Jadida, Chouaib Doukkali University, El Jadida, Morocco. e-mail: habibhassouni85@gmail.com

Oumaima Aarabate
Laboratory of Fundamental Mathematics and their Applications, Department of Mathematics, Faculty of Sciences El Jadida, Chouaib Doukkali University, El Jadida, Morocco. e-mail: oumaimaaarabate@gmail.com

Omar Balatif
Laboratory of Fundamental Mathematics and their Applications, Department of Mathematics, Faculty of Sciences El Jadida, Chouaib Doukkali University, El Jadida, Morocco. e-mail: balatif.maths@gmail.com

How to cite this article
Belhdid, S., Hassouni, H., Aarabate, O. and Balatif, O., Behavioral modeling and control strategies for Rumor-induced customer dynamics on digital platforms. *Iran. J. Numer. Anal. Optim.*, 2027; 17(1): 72-108. https://doi.org/10.22067/ijnao.2026.96859.1794

number $\mathcal{R}_0$ is derived via the next-generation matrix method and is used to characterize the stability of the rumor-free and endemic equilibria. Both local and global stability analyses are carried out using linearization and Lyapunov methods, respectively. An optimal control problem is then formulated with two time-dependent intervention strategies: Incentive-based and support-based controls. The existence of optimal controls is verified, and the necessary optimality conditions are derived via Pontryagin's maximum principle. Numerical simulations based on a forward-backward sweep scheme illustrate the effectiveness of the proposed strategies in reducing hesitation and enhancing long-term customer loyalty, with combined interventions yielding the best results.

AMS subject classifications (2020): Primary 49J20; Secondary 34D20.

Keywords: Compartmental models; Optimal control; Rumors; Customer behavior; Numerical simulations; Digital platforms.

1 Introduction

Rumor dissemination on digital platforms profoundly influences customer behavior, shaping perceptions, trust, and engagement within online ecosystems. In today's hyperconnected environment, false or misleading information can spread rapidly, much like infectious diseases, thereby affecting how potential users transition toward or away from loyalty. Understanding and mitigating these rumor-induced behavioral dynamics have become essential for maintaining the sustainability and credibility of digital platforms.

This study investigates the interplay between rumor propagation and customer behavioral dynamics through a compartmental mathematical model that distinguishes among potential, hesitant, and loyal customers. Drawing from epidemiological modeling frameworks, we analyze how information diffusion, specifically the spread of tumor, affects customer conversion, hesitation, and retention processes [18]. By formulating the problem in this manner, the model captures the contagion-like properties of rumor dissemination and enables the development of optimal control strategies to mitigate its adverse effects while enhancing user engagement [20, 22].

The theoretical foundation of this research is based on classical and contemporary rumor spreading models, which treat the dissemination of information as analogous to the spread of infectious diseases. These models have evolved to incorporate key behavioral and cognitive factors such as education, debunking efforts, and intervention strategies, highlighting their role in reducing misinformation persistence [18, 21]. Several studies have also accounted for individual heterogeneity, distinguishing among those who propagate rumors, those who identify or refute

them, and those who remain indifferent, thereby offering a more realistic portrayal of social communication processes [18, 14].

Recent advances in compartmental modeling and optimal control have highlighted their utility in analyzing complex social and behavioral dynamics. In particular, the application of SIR models to information and rumor diffusion has grown substantially [18, 6, 25, 27], with several studies demonstrating the importance of control-theoretic approaches in managing misinformation [9, 4, 19]. These works collectively establish the mathematical foundation on which the present study builds, while our contribution lies in extending this framework to a customer behavioral context with an explicit hesitancy compartment. For example, El Bhih et al. [9] developed a framework to study the spread of rumors and counter-rumors on social networks, formulating multiple equilibria and designing optimal interventions using Pontryagin's maximum principle to influence collective behavior. Similarly, studies on scam rumor propagation have employed deterministic models combined with cost-effectiveness analysis to evaluate strategies for mitigating false information on social platforms, emphasizing the efficiency of targeted interventions [4]. In the context of epidemiology, Laaroussi, El Bhih, and Rachik [15] demonstrated how optimal vaccination and treatment policies can be formulated under constrained resources for a multi-strain SEIR model of COVID-19, providing insight into balancing limited resources while achieving maximal impact. Furthermore, Yaagoub, El Bhih, and Allali [26] introduced a fractional-order infection model for computer virus propagation, illustrating how memory effects and fractional dynamics can improve the realism and predictive power of compartmental models. Collectively, these studies underscore the versatility of compartmental and optimal control approaches for understanding the evolution of complex systems and designing effective intervention strategies. Inspired by these works, our study applies a similar framework to investigate merchants' adoption of e-commerce, where the dynamics of acceptance and refusal can be influenced through targeted control measures. However, most existing works rely on simplified tow-state models, typically classifying individuals as either active or inactive spreaders of information [12]. While analytically tractable, such models overlook the behavioral nuances and decision-making diversity inherent in customer interactions on digital platforms. In contrast, recent studies emphasize that users exhibit varying degrees of commitment and susceptibility ranging from potential adopters who are exploring the platform to hesitant users influenced by rumors, to loyal customers who reinforce platform stability [11, 2].

The present work addresses this gap by proposing a multi-compartmental behavioral model that explicitly differentiates these customer categories and incorporates the effect of rumor propagation on their transitions. This approach aligns with recent advances in information diffusion and population dynamics modeling, which account for delays, cross-transmission, and endogenous attention mechanisms [3, 7]. Furthermore, the model recognizes that algorithmic recom-

mendation systems can inadvertently amplify misinformation by promoting highly engaging but unreliable content, thereby reinforcing hesitancy among potential users [13].

In competitive digital environments, media competition and attention-driven algorithms may unintentionally fuel the spread of misinformation, undermining both user trust and long-term platform growth [1]. To confront these challenges, our study integrates behavioral modeling, rumor propagation dynamics, and optimal control theory into a single mathematical framework. By doing so, it seeks to analyze the stability properties of the system and design effective control strategies such as rumor refutation campaigns or customer education initiatives that can enhance platform resilience.

Ultimately, this research contributes to the growing body of work that applies mathematical modeling and control theory to social and behavioral systems. By coupling rumor dynamics with customer segmentation, the proposed model provides a deeper understanding of how misinformation influences user transitions and engagement. The resulting insights offer both theoretical and practical guidance for platform managers and policymakers aiming to balance information flow, customer loyalty, and sustainable growth in the digital era [8].

The proposed model offers three key advantages over existing approaches. First, unlike classical two-state rumor models that classify individuals simply as spreaders or ignorant, our model captures the intermediate *hesitant* state, which is empirically more realistic for customer behavior on digital platforms where indecision is prevalent. Second, the use of frequency-dependent interaction rather than mass-action kinetics ensures that the model remains well posed as the total population varies over time. Third, the integration of two distinct and complementary optimal control strategies: incentive-based and support-based allows for a richer intervention design than a single-control formulation, while Pontryagin's maximum principle provides a rigorous and tractable characterization of optimal policies.

The remainder of the paper is structured as follows. Section 2 introduces the proposed multi-compartmental model, detailing the dynamics of potential, hesitant, and loyal customers and the mechanisms of rumor propagation. Section 3 is dedicated to the mathematical analysis of the model, including the study of equilibrium points, stability properties, and the basic reproduction number. Section 4 formulates the optimal control problem, defining admissible strategies, objective functionals, and the associated existence results. Additionally, it drives the necessary conditions for optimality using Pontryagin's maximum principle and presents the characterization of the optimal controls. Section 5 provides numerical simulations to illustrate the effectiveness of the control strategies under various scenarios and sensitivity analyses of key parameters. Finally, Section 6 concludes the paper with a discussion of the main findings, practical implications, and potential directions for future research.

2 Mathematical model overview:

The dynamical system under consideration describes the interaction and engagement dynamics of users on a digital platform. Three distinct compartments encapsulate the diverse user categories: Potential customers ($P(t)$), loyal customers ($L(t)$), and hesitant customers ($H(t)$). Each compartment represents a specific phase in the user journey, from potential consideration to active engagement or hesitancy. The model accounts for the interplay between these compartments, considering factors such as attraction, conversion, retention, and natural attrition. This detailed analysis aims to shed light on the complex dynamics influencing user engagement, offering valuable insights for optimizing and enhancing the digital platform's user experience. The model variables are summarized in Table 1.

Table 1: Description of the model variables

$P(t)$	Potential customers or users considering the digital platform.
$L(t)$	Loyal customers who actively engage with the digital platform.
$H(t)$	Hesitant customers who are interested but not fully engaged.

Potential customers ($P(t)$):

This compartment represents individuals who are in the consideration phase, pondering the use of the digital platform. Attraction occurs at a rate Ω_1, reflecting the platform's appeal. Interactions play a crucial role, with potential customers converting to loyal customers ($\beta_1 P(t)L(t)$) or hesitant customers ($\beta_2 P(t)H(t)$), influenced by the existing user base. Natural attrition (μ) accounts for potential customers naturally disengaging. The overall dynamic process involves a delicate balance between attraction, conversion to loyalty, conversion to hesitancy, and the inherent attrition rate.

Loyal customers ($L(t)$):

This compartment represents actively engaged users who have transitioned from potential customers. The dynamic process is shaped by the conversion of potential customers to loyal customers ($\beta_1 P(t)L(t)$), their own retention (α_1), and the conversion of loyal customers to hesitant ones (π). Retention (α_1) captures the platform's ability to retain potential customers as loyal users. The conversion dynamics involve both attracting new users and converting loyal users to hesitant ones. Natural attrition (μ) also affects this group, reflecting the natural disengagement of loyal users from the platform.

Hesitant customers ($H(t)$):

This compartment represents individuals intrigued by the platform but not fully committed. The dynamic process involves potential customers converting to hesitant customers ($\beta_2 P(t)H(t)$), their own retention (α_2), and the conversion of hesitant customers to loyal ones (τ). Retention (α_2) signifies the platform's ability to retain potential customers as hesitant users. The conversion dynamics reflect the interplay between attracting new hesitant users and converting hesitant users to loyal ones. Natural attrition (μ) affects hesitant customers similarly to loyal customers. The overall dynamic process encompasses attraction, conversion to loyalty, conversion to hesitancy, and the inherent attrition rate, contributing to a comprehensive analysis of user engagement on the digital platform. The corresponding compartmental flow diagram is depicted in Figure 1, and the resulting dynamics are governed by the following system of ordinary differential equations:

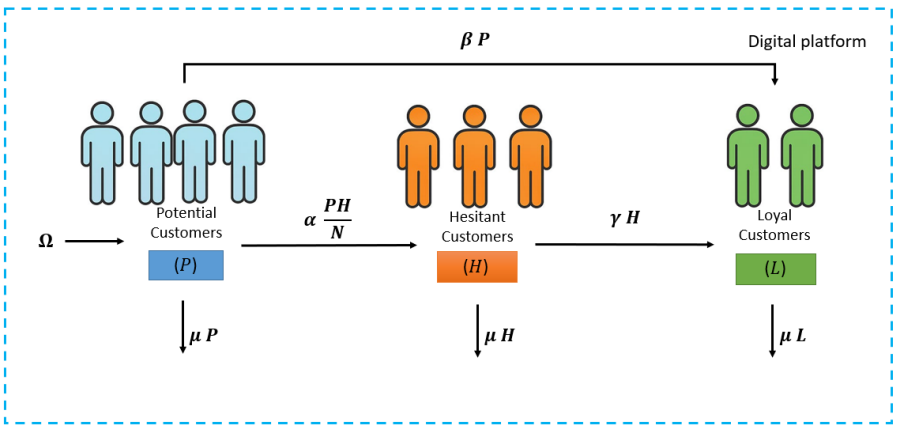

Figure 1: The compartmental flow diagram for the customers spreading process.

$$
\begin{aligned}
\frac{dP(t)}{dt} &= \Omega - \alpha\frac{P(t)H(t)}{N} - (\beta+\mu)P(t),\\
\frac{dH(t)}{dt} &= \alpha\frac{P(t)H(t)}{N} - (\gamma+\mu)H(t),\\
\frac{dL(t)}{dt} &= \beta P(t) + \gamma H(t) - \mu L(t),
\end{aligned}
\tag{1}
$$

with the initial conditions

$$P(0) \geq 0, \quad L(0) \geq 0, \quad H(0) \geq 0.$$

Parameters	Meaning
Ω	Attraction or onboarding rate of potential customers to the platform.
β	Conversion rate from potential to loyal customers.
α	Conversion rate from potential to hesitant customers.
μ	Natural loss rate of customers (attrition rate).
γ	Rate at which hesitant customers become loyal customers.

3 Model analysis

3.1 Positivity and boundedness

Considering the model system (1), we provide the following:

$$\left.\frac{dP}{dt}\right|_{\{P=0,\ H>0,\ L>0\}} = \Omega > 0,$$
$$\left.\frac{dH}{dt}\right|_{\{P>0,\ H=0,\ L>0\}} = 0,$$
$$\left.\frac{dL}{dt}\right|_{\{P>0,\ H>0,\ L=0\}} = \beta P + \gamma H > 0.$$

Observing that all rates are nonnegative at the boundary of the nonnegative cone in $\mathbb{R}^3$, and considering the inward directions of the vector fields on these boundaries, initiating the system from any interior point of this cone guarantees that the solutions will persist within the cone indefinitely. This guarantees the positivity of all populations in the system over time.

Theorem 1. The set $\Theta = \{(P, H, L) \in \mathbb{R}^3_+ : 0 \leq P + L + H \leq \frac{\Omega}{\mu}\}$ with the initial conditions $P(0) \geq 0,\ L(0) \geq 0,\ H(0) \geq 0$, is a positively invariant and global attractive set under the system (1).

Proof. Note that the total population N is given by $N = P + L + H$. Differentiating, we obtain that

$$\frac{dN}{dt} = \Omega - \mu N,$$

thereafter, by solving the rate equation we get the solution $N(t)$ as follows:

$$N(t) = \frac{\Omega}{\mu} - \left(\frac{\Omega}{\mu} + N(0)\right) \exp^{-\mu t}. \tag{2}$$

If $N(t) > \frac{\Omega}{\mu}$, then from (2), we observe that $\lim_{t\to\infty} N(t) = \frac{\Omega}{\mu}$. If $N(0) \leq \frac{\Omega}{\mu}$, then $N(t) \leq \frac{\Omega}{\mu}$. This shows that all solutions with initial conditions in Θ stay in Θ for all future times, and consequently the set Θ is a positively invariant for the system (1). Therefore, we get to the conclusion that the set Θ is a positively invariant set and globally attractive for the model system (1).

□

Remark 1. Adding the three equations of system (1), the total population $N(t) = P(t)+H(t)+L(t)$ satisfies

$$\frac{dN}{dt} = \Omega - \mu N(t),$$

whose explicit solution is

$$N(t) = \frac{\Omega}{\mu} - \left(\frac{\Omega}{\mu} - N(0)\right) e^{-\mu t}.$$

Therefore, $N(t)$ is not constant in general; it varies over time unless $N(0) = \Omega/\mu$ exactly. However, $N(t)$ is bounded and converges asymptotically to Ω/μ as $t \to \infty$, regardless of $N(0)$. This justifies the use of the time-varying $N(t)$ in the frequency-dependent interaction term $\alpha P(t)H(t)/N$, which normalizes the rumor contact rate by the current total population, consistent with standard compartmental modeling conventions. In the numerical simulations, $N(t)$ is updated at each time step of the discretization scheme.

3.2 Existence of free-equilibrium point and Basic reproduction number

The free-equilibrium point is computed by equating the right-hand side of the system (1) to zero, that is,

$$\frac{dP(t)}{dt} = 0, \quad \frac{dH(t)}{dt} = 0, \quad \frac{dL(t)}{dt} = 0. \tag{3}$$

Therefore, the free-equilibrium steady state of the model (1) is the state in which there are no loyal customers and no hesitant customers into the total population, that is,

$$H(t) = 0, \quad L(t) = 0.$$

Thus, after equating the right-hand side of the system (1) to zero and substituting these values into the system, we get

$$\Omega - (\beta + \mu)P = 0 \quad \Longrightarrow P^* = \frac{\Omega}{\beta + \mu},$$

and

$$\beta P - \mu L = 0 \quad \Longrightarrow L^* = \frac{\beta\Omega}{\mu(\beta + \mu)}.$$

Consequently, the free-equilibrium $\mathcal{E}_f$ is given by

$$\mathcal{E}_f = \left\{ (P^*, 0, L^*) : \left(\frac{\Omega}{\beta + \mu}, 0, \frac{\beta\Omega}{\mu(\beta + \mu)} \right) \right\}, \tag{4}$$

which always exists.

We now derive the basic reproduction number $\mathcal{R}_0$ of the model (1), given by the following theorem.

Theorem 2. The basic reproduction number of the model system (1) is stated as follows:

$$\mathcal{R}_0 = \alpha \frac{\mu}{(\beta + \mu)(\gamma + \mu)}, \tag{5}$$

Proof. Use the next generation matrix [24]. Let $X = (P, H, L)$; then system can be written

$$\frac{dX}{dt} = f(X) - v(X),$$

where

$$f(X) = \begin{pmatrix} \frac{\alpha PH}{N} \\ 0 \\ 0 \end{pmatrix},$$

and

$$v(X) = \begin{pmatrix} (\gamma + \mu) H \\ -\beta P - \gamma H + \mu L \\ -\Omega + \frac{\alpha PH}{N} + (\beta + \mu) P \end{pmatrix}.$$

Then, the two Jacobian matrices at the free-equilibrium point for $f(X)$ and $v(X)$ are written as follows:

$$J\left(f\left(\mathcal{E}_f\right)\right) = \begin{pmatrix} F_{2\times 2} & 0 \\ & 0 \\ 0 & 0\ 0 \end{pmatrix},$$

and

$$J\left(v\left(\mathcal{E}_f\right)\right) = \begin{pmatrix} V_{2\times 2} & 0 \\ & -\beta \\ \dfrac{\mu\alpha}{(\beta+\mu)} & 0\ \ 0 \end{pmatrix},$$

with

$$F_{2\times 2} = \begin{pmatrix} \alpha\frac{\mu}{\beta+\mu} & 0 \\ 0 & 0 \end{pmatrix},$$

and

$$V_{2\times 2} = \begin{pmatrix} (\gamma+\mu) & 0 \\ -\gamma & \mu \end{pmatrix}.$$

Thereafter, by a simple calculation we get the following:

$$\mathcal{R}_0 = \rho(F_{2\times 2}V_{2\times 2}^{-1}) = \alpha\frac{\mu}{(\beta+\mu)(\gamma+\mu)}.$$

□

Remark 2. In the context of the compartmental model describing customer behavior on digital platforms, the basic reproduction number $\mathcal{R}_0$ represents the expected number of new hesitant customers generated by one hesitant customer in the absence of other influences. Specifically, $\mathcal{R}_0$ is a threshold parameter that helps determine the potential for customer base growth. If $\mathcal{R}_0 > 1$, each potential customer, on average, leads to more than one hesitant customer, indicating that the platform's customer base is likely to grow. Conversely, if $\mathcal{R}_0 < 1$, the platform struggles to convert potential customers into hesitant ones at a sufficient rate, suggesting that the customer base may decline over time. Understanding $\mathcal{R}_0$ helps the platform strategize its marketing and engagement efforts to ensure sustainable growth and transition towards a stable, loyal customer base.

3.3 Sensitivity analysis in Rumor-induced customer dynamics

Sensitivity analysis serves as a pivotal tool to identify and quantify the impact of key model parameters on the prevalence of hesitant customers and the overall influence of rumors within digital platforms. In the context of our study, the basic reproduction number R_0 plays a crucial role, characterizing the potential for rumor-induced transitions among customer segments. Understanding how variations in model parameters affect R_0 provides insights into the dynamics of potential, hesitant, and loyal customers, thereby informing strategies to mitigate the adverse effects of misinformation [6, 19].

In this section, we examine the effect of each parameter in system (1) on the value of R_0. To determine which parameters most significantly drive the spread of rumor-induced hesitation and affect customer conversion to loyalty, a sensitivity analysis is conducted following the approaches in [25, 27]. Specifically, we compute the partial derivatives of R_0 with respect to the system parameters in (1) to obtain the corresponding sensitivity indices (S.Is.), providing a quantitative measure of each parameter's influence on the dynamics of potential, hesitant, and loyal customers.

This analysis not only enhances our understanding of the model's behavior but also aids in identifying critical parameters that can be targeted to control the spread of rumors and promote customer loyalty. By focusing on these influential parameters, digital platforms can develop more effective strategies to manage misinformation and its impact on user engagement [19, 6].

Definition 1. The S.I. $Z_q^{R_0}$ of the basic reproduction number R_0, varying with parameter q, is defined as

$$Z_q^{R_0} = \frac{\partial R_0}{\partial q} \cdot \frac{q}{R_0},$$

where $\frac{\partial R_0}{\partial q}$ denotes the partial derivative of R_0 with respect to q.

Specifically, the computed S.Is. of the basic reproduction number R_0 with respect to the parameters of the controlled PHL system are as follows:

$$\begin{cases} \Upsilon_{\mu}^{R_0} = \dfrac{\partial R_0}{\partial \mu} \cdot \dfrac{\mu}{R_0} = \dfrac{\gamma\beta - \mu^2}{(\gamma+\mu)(\beta+\mu)}, \\ \Upsilon_{\alpha}^{R_0} = \dfrac{\partial R_0}{\partial \alpha} \cdot \dfrac{\alpha}{R_0} = 1, \\ \Upsilon_{\beta}^{R_0} = \dfrac{\partial R_0}{\partial \beta} \cdot \dfrac{\beta}{R_0} = -\dfrac{\beta}{\beta+\mu}, \\ \Upsilon_{\gamma}^{R_0} = \dfrac{\partial R_0}{\partial \gamma} \cdot \dfrac{\gamma}{R_0} = -\dfrac{\gamma}{\gamma+\mu}. \end{cases}$$

These indices quantify the relative impact of each parameter on the reproduction number, providing insight into which factors most strongly influence the spread of hesitant (H) and loyal (L) customer behaviors. The corresponding numerical values, computed at the nominal parameter set, are reported in Table 2. These results are visualized in Figure 2, which displays the S.Is. of R_0 with respect to each parameter.

Table 2: Sensitivity of the basic reproduction number R_0 to parameter perturbations (nominal values: $\alpha = 5.0 \times 10^{-4}$, $\beta = 1.0 \times 10^{-4}$, $\gamma = 5.0 \times 10^{-6}$, $\mu = 3.0 \times 10^{-4}$).

Parameter	Nominal value	S.I. $Z_q^{R_0}$	R_0 (+10%)	ΔR_0 (+10%) (percent)
α	5.00×10^{-4}	1.0000	1.3525	+10.00%
β	1.00×10^{-4}	−0.2500	1.1995	−2.44%
γ	5.00×10^{-6}	−0.01639	1.2275	−0.16%
μ	3.00×10^{-4}	−0.73361	1.1454	−6.84%

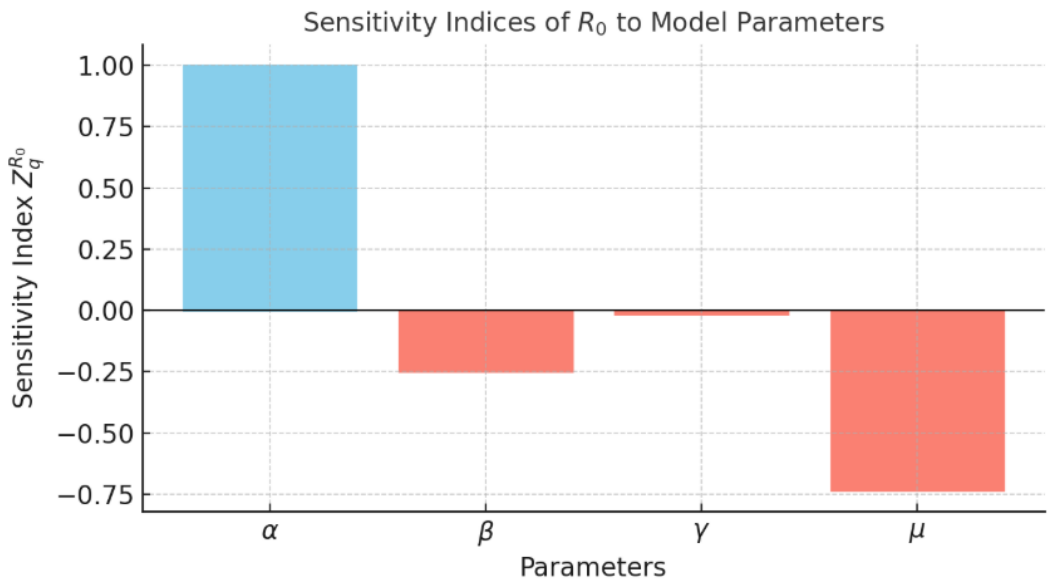

Figure 2: Sensitivity analysis of the parameters.

3.4 Existence of an endemic steady state

The model system (1) admits *two* distinct equilibrium points: The rumor-free equilibrium $\mathcal{E}_f$ (established in Section 3.2), which exists for all parameter values, and the endemic equilibrium E_e^* described below, which exists and is biologically meaningful only when $\mathcal{R}_0 > 1$.

The endemic equilibrium point in this customer behavior model toward digital platforms represents a stable state where the proportions of potential, hesitant, and loyal customers remain constant over time. At this point, the rates of transitions between the compartments (potential to hesitant, hesitant to loyal, etc.) balance each other out, resulting in no net changes in the number of customers in each compartment. This equilibrium reflects a situation where the digital platform has reached a steady state in customer dynamics, with consistent engagement and retention patterns. Understanding this equilibrium can help the platform predict long-term customer behavior and design strategies to maintain or shift this balance in the desired directions. Therefore, the endemic-steady state for our model is given by the following:

$$E_e^* = (P^*, H^*, L^*)\,,$$

where

$$P^* = \Omega \frac{(\gamma + \mu)}{\mu\alpha},$$

$$H^* = \Omega \frac{(\beta + \mu)(\mathcal{R}_0 - 1)}{\mu\alpha},$$

and

$$L^* = \frac{\beta\Omega^2(\gamma + \mu)^2 + \gamma\Omega(\beta + \mu)(\gamma + \mu)}{\mu\alpha(\gamma + \mu)} (\mathcal{R}_0 - 1).$$

3.5 Local stability analysis of the steady states

Theorem 3. Considering the system model (1) at the free-equilibrium $\mathcal{E}_f$, it is locally asymptotically stable if $\mathcal{R}_0 < 1$, and unstable when $\mathcal{R}_0 > 1$.

Proof. We compute the Jacobian of system (1) evaluated at $\mathcal{E}_f$:

$$J(\mathcal{E}_f) = \begin{bmatrix} -\beta - \mu & -\alpha\frac{\mu}{\beta+\mu} & 0 \\ 0 & (R_0 - 1)(\gamma + \mu) & 0 \\ \beta & \gamma & -\mu \end{bmatrix}.$$

Therefore, the eigenvalues of the characteristic equation of $J(\mathcal{E}_f)$ are
$v_1 = (R_0 - 1)(\gamma + \mu) < 0,$
$v_2 = -\mu < 0,$
$v_3 = -\beta - \mu < 0.$

Therefore, all the eigenvalues of the characteristic equation are negative if $R_0 < 1$. Hence, the equilibrium point $\mathcal{E}_f$ is locally asymptotically stable if $R_0 < 1$ and unstable if $R_0 > 1$.

□

Theorem 4. If $R_0 > 1$, the endemic equilibrium E_e^* is locally asymptotically stable.

Proof. Let us consider the endemic equilibrium point E_e^*, given by

$$X_* = \left(\frac{\Omega}{\alpha\mu}(\gamma + \mu), \left(\frac{\Omega}{\alpha\mu}(R_0 - 1)(\beta + \mu)\right), \frac{1}{\alpha\mu^2}(\Omega\beta\mu + \Omega\beta\gamma R_0 + \Omega\gamma\mu(R_0 - 1))\right).$$

Then the Jacobian matrix at E_e^* is given as follows:

$$J(E_e^*) = \begin{bmatrix} -\alpha\frac{H^*}{N} - (\beta + \mu) & -\alpha\frac{P^*}{N} & 0 \\ \alpha\frac{H^*}{N} & \alpha\frac{P^*}{N} - (\gamma + \mu) & 0 \\ \beta & \gamma & -\mu \end{bmatrix},$$

and its characteristic equation is

$$X^3 + a_2X^2 + a_1X + a_0 = 0,$$

where

$$a_2 = \frac{\mu\alpha}{(\beta+\mu)} + \mu,$$
$$a_1 = \frac{\mu^2\alpha}{(\beta+\mu)} + (\beta+\mu)(\gamma+\mu)\left(R_0 - 1\right),$$
$$a_0 = \frac{\mu^3\alpha}{(\beta+\mu)N} + \mu(\beta+\mu)(\gamma+\mu)\left(R_0 - 1\right).$$

By the Routh–Hurwitz criterion, system (1) is locally asymptotically stable if $a_2 > 0$, $a_0 > 0$, and $a_2a_1 > a_0$. Thus, E_e^* is locally asymptotically stable if $R_0 > 1$. □

3.6 Global stability analysis

Now, we are concerned with the global asymptotic stability of free equilibrium $\mathcal{E}_f$ and endemic equilibrium E_e^* of model (1), respectively.

Theorem 5. The free equilibrium $\mathcal{E}_f$ is globally asymptotically stable on Θ, if $R_0 \leq 1$.

Proof. To prove the global stability of the free equilibrium $\mathcal{E}_f$, we consider the Lyapunov function constructed as follows: $V : \Omega \to \mathbb{R}$ given by

$$V(P,H) = \frac{1}{2}\left((P-P_0)+H\right)^2 + \frac{(\beta+\gamma+2\mu)}{\alpha}NH.$$

Then, the time derivative of V is

$$\begin{aligned}
V'(P,H) &= \big((P-P_0)+H\big)\big(P'+H'\big) + \frac{\beta+\gamma+2\mu}{\alpha}NH', \\
&= \Bigg(\Big(P - \frac{\Omega}{\beta+\mu} + H\Big)\Big(\Omega - \frac{\alpha PH}{N} - (\beta+\mu)P + \frac{\alpha PH}{N} - (\gamma+\mu)H\Big) \\
&\quad + \frac{\beta+\gamma+2\mu}{\alpha}N\Big(\frac{\alpha PH}{N} - (\gamma+\mu)H\Big)\Bigg), \\
&= -(\beta+\mu)\Big(P - \frac{\Omega}{\beta+\mu}\Big)^2 - (\gamma+\mu)H^2 \\
&\quad - (\beta+\gamma+2\mu)\frac{\gamma+\mu}{\alpha}N(1-R_0)H.
\end{aligned}$$

Thus, $V^{'}(P,H) \leq 0$ for $R_0 \leq 1$.
In addition, If $R_0 \leq 1$, then $V'(P,H) = 0 \iff P = P_0$ and $H = 0$.

Hence, by LaSalle's invariance principle [16], the free equilibrium point $\mathcal{E}_f$ is globally asymptotically stable on Θ. □

Theorem 6. The endemic equilibrium E_e^* is globally asymptotically stable on Θ, if $R_0 > 1$.

Proof. To prove the global stability of the endemic equilibrium E_e^*, we consider the Lyapunov function constructed as follows: $V : \Omega \to \mathbb{R}$ given by

$$V(P,H) = C_1\left(P - P^* \ln\frac{P}{P^*}\right) + C_2\left(H - H^* \ln\frac{H}{H^*}\right),$$

where C_1 and C_2 are positive constants to be chosen later. Then, the time derivative of the Lyapunov function is given by

$$V^{'}(P,H) = \frac{\alpha}{N}\left(C_2 - C_1\right)\left(H - H^*\right)\left(P - P^*\right) - \Omega C_1 \frac{(P-P^*)^2}{PP^*}.$$

For $C_1 = C_2 = 1$, we get

$$V^{'}(P,H) = -\Omega\frac{(P-P^*)^2}{PP^*} \leq 0,$$

we also get

It remains to identify the largest invariant set contained in $\mathcal{M} = \{(P,H) \in \Theta : V'(P,H) = 0\} = \{(P,H) \in \Theta : P = P^*\}$. On this set, $\dot{P} = 0$, so the first equation of system (1) gives $\Omega - \alpha P^* H/N - (\beta+\mu)P^* = 0$. Since at the endemic equilibrium $\Omega = \alpha P^* H^*/N + (\beta+\mu)P^*$, substituting yields $\alpha P^*(H - H^*)/N = 0$, and hence $H = H^*$. Therefore, the largest invariant subset of $\mathcal{M}$ is the singleton $\{E_e^*\}$.

$V^{'}(P,H) = 0 \iff P = P^*$.

Hence, by LaSalle's invariance principle [16], the endemic equilibrium point E_e^* is globally asymptotically stable on Θ. □

4 Optimal control problem

The current section is devoted to the model's optimal control analysis. By implementing two time-dependent controls $v(t)$ and $w(t)$ to our proposed system (1), we obtain the following controlled dynamical system governed by the upcoming differential equations:

$$\frac{dP(t)}{dt} = \Omega - \alpha\frac{P(t)H(t)}{N} - (\beta+\mu)P(t) - v(t)P(t),$$

$$\begin{aligned}\frac{dH(t)}{dt} &= \alpha\frac{P(t)H(t)}{N} - (\gamma+\mu)H(t) - w(t)H(t),\\ \frac{dL(t)}{dt} &= \beta P(t) + \gamma H(t) - \mu L(t) + v(t)P(t) + w(t)H(t),\end{aligned} \tag{6}$$

with the initial conditions

$$P(0) \geq 0, \quad L(0) \geq 0, \quad H(0) \geq 0.$$

Taking into consideration the economic and ethical restrictions of the digital platforms, the intervention policies must be restricted. Consequently, the two controls have to be taken as bounded in $[0, 1]$. The control strategies $v(t)$ and $w(t)$ are relevant precisely when $\mathcal{R}_0 > 1$, that is, when the rumor-free equilibrium $\mathcal{E}_f$ is unstable and the system tends toward the endemic equilibrium E_e^*. When $\mathcal{R}_0 \leq 1$, the uncontrolled system already converges to $\mathcal{E}_f$ (see Theorem 5), and no intervention is required. The optimal controls are therefore designed to drive the system back toward a low-hesitancy state when the reproduction number exceeds the critical threshold.

1. **Incentive-based control strategy** $v(t)$ is a strategy used in various fields, such as economics, environmental management, and public health, to influence the behavior of individuals or groups by offering rewards or penalties. The underlying idea is to align individual motivations with broader societal goals by creating incentives that encourage desirable actions while discouraging harmful ones. For example, in environmental management, incentives like tax credits or subsidies may be offered to companies that reduce pollution, while fines or higher taxes might be imposed on those that exceed pollution limits. In public health, similar strategies can be applied, such as offering financial incentives to people who engage in healthy behaviors or penalizing risky behaviors that contribute to public health issues. Incentive-based control leverages human motivation to drive change without relying solely on direct regulations or restrictions, allowing for flexibility and innovation in achieving desired outcomes.

2. **Support-based control strategy** $w(t)$ focuses on providing resources, tools, or assistance to individuals or organizations to help them achieve desired behaviors or outcomes. Rather than using incentives or penalties, these strategies aim to empower and enable change through guidance, education, or infrastructural support. In environmental management, for instance, support-based strategies might involve offering technical assistance or providing access to renewable energy technologies to help businesses reduce emissions. In public health, these strategies could include offering free healthcare services, counseling, or educational programs to promote healthier lifestyles. By addressing barriers to positive behavior, such as lack of knowledge, resources, or access support-based control strategies

foster an environment where individuals and groups can make sustainable changes. This approach tends to be collaborative and often works best when paired with other control mechanisms, like regulations or incentive-based programs, to encourage long-term compliance and growth.

In summary, this section has formulated the optimal control problem for the proposed PHL system by introducing two time-dependent interventions: The incentive-based control $v(t)$ and the support-based control $w(t)$. Both controls are bounded to respect practical and ethical constraints, reflecting realistic implementation scenarios. The incentive-based strategy targets behavior modification through rewards or penalties, while the support-based strategy provides resources and assistance to facilitate positive outcomes. Together, these controls establish a flexible and practical framework for designing intervention policies that aim to optimize system performance while adhering to societal and economic considerations. This formulation lays the foundation for the subsequent analysis, including the existence of optimal controls, derivation of necessary conditions, and numerical simulations to evaluate their effectiveness.

4.1 Objective functional

We aim to minimize the following objective functional:

$$J(v,w) = H(t_f) - L(t_f) + \int_{t_0}^{t_f} \Big[H(t) - L(t) + \frac{M_1}{2}v^2(t) + \frac{M_2}{2}w^2(t)\Big]dt, \tag{7}$$

where t_f is the final time and $M_1, M_2 > 0$ are cost coefficients that weigh the relative importance of the controls v and w.

We search for optimal controls (v^*, w^*) such that

$$J(v^*, w^*) = \min_{(v,w)\in U_{ad}^2} J(v,w),$$

with the admissible control set

$$U_{ad} = \{u(t) : 0 \le u(t) \le 1,\ t \in [t_0, t_f]\}.$$

From a broader perspective, the objective functional is designed to manage the trade-off between converting hesitant customers, represented by $H(t)$, into more loyal behavior, and preserving the existing loyal customer base, represented by $L(t)$. At the same time, it incorporates the

cost of implementing the incentive-based and support-based control strategies $v(t)$ and $w(t)$ through the weighting coefficients M_1 and M_2, ensuring that interventions remain both effective and feasible within practical economic constraints. By restricting the admissible controls to the interval $[0, 1]$, we reflect realistic limitations on the intensity of policy implementation. This formulation provides a rigorous approach for deriving optimal strategies that encourage hesitant customers to engage positively with the system while safeguarding the loyalty of established customers. Moreover, it sets the foundation for numerical simulations to evaluate the impact of different combinations of incentives and support measures on customer dynamics and overall system performance.

4.2 Existence of optimal controls

Fleming and Rishel's result (see [10, Corollary 4.1]) can be used to determine whether the optimal controls exist.

Theorem 7. Consider the controlled PHL system

$$\begin{cases} \dot{P}(t) &= \Omega - \dfrac{\alpha P(t)H(t)}{N} - (\beta+\mu)P(t) - v(t)P(t), \\ \dot{H}(t) &= \dfrac{\alpha P(t)H(t)}{N} - (\gamma+\mu)H(t) - w(t)H(t), \\ \dot{L}(t) &= \beta P(t) + \gamma H(t) - \mu L(t) + v(t)P(t) + w(t)H(t), \end{cases}$$

with initial conditions $P(0) \geq 0$, $H(0) \geq 0$, and $L(0) \geq 0$, and the objective functional

$$J(v,w) = H(t_f) - L(t_f) + \int_{t_0}^{t_f} \Big[H(t) - L(t) + \frac{M_1}{2}v^2(t) + \frac{M_2}{2}w^2(t)\Big]dt.$$

Then, there exists an optimal control $(v^*, w^*) \in U_{ad}^2$ such that

$$J(v^*, w^*) = \min_{(v,w)\in U_{ad}^2} J(v,w),$$

provided that all the following conditions hold:

1. The set of corresponding state variables and admissible controls is nonempty.

2. The control set U_{ad} is closed and convex.

3. A linear function in the state and control variables bounds the right-hand side of the state system.

4. The integrand $L(P,H,L,v,w) = H - L + \frac{M_1}{2}v^2 + \frac{M_2}{2}w^2$ of the objective functional is convex on U_{ad}, and there exist constants $c_1, c_2 > 0$ and $\epsilon > 1$ such that

$$L(P,H,L,v,w) \geq -c_1 + c_2\left(|v|^2 + |w|^2\right)^{\epsilon/2}.$$

Proof. **Condition 1.** We must show that for any $(v,w) \in U_{\text{ad}}^2$, the controlled state system admits a unique solution on $[t_0, t_f]$. We use a simplified version of an existing result (see [5, Theorem 7.1.1]).
Let

$$\dot{P} = O_P(t;P,H,L), \quad \dot{H} = O_H(t;P,H,L), \quad \dot{L} = O_L(t;P,H,L),$$

where O_P, O_H, and O_L denote the right-hand sides of the controlled PHL system.

Set the controls $v(t) = c_1$ and $w(t) = c_2$ as constants. Since all parameters are constants, and P, H, and L are continuous, the functions O_P, O_H, and O_L are continuous.
Moreover, the partial derivatives

$$\frac{\partial O_P}{\partial P}, \frac{\partial O_P}{\partial H}, \frac{\partial O_P}{\partial L}, \quad \frac{\partial O_H}{\partial P}, \frac{\partial O_H}{\partial H}, \frac{\partial O_H}{\partial L}, \quad \frac{\partial O_L}{\partial P}, \frac{\partial O_L}{\partial H}, \frac{\partial O_L}{\partial L}$$

are all continuous. Since $N(t) \geq N(0)e^{-\mu t} > 0$ for all finite t (by the positivity established in Section 3), the nonlinear term $\alpha PH/N$ is smooth and the Lipschitz condition is satisfied locally on $\mathbb{R}_+^3$. Consequently, by the Picard–Lindelöf theorem, there exists a unique solution (P,H,L) satisfying the initial conditions. Moreover, by Theorem 1, this solution remains in the bounded invariant set Θ for all $t \in [t_0, t_f]$.
Therefore, the set of state variables and controls is nonempty, and Condition 1 is satisfied.

Condition 2. By the definition, U_{ad} is closed. Let $v_1, v_2 \in U_{ad}$ and $\varepsilon \in [0,1]$; then

$$0 \leq \varepsilon v_1 + (1-\varepsilon)v_2.$$

Since $\varepsilon v_1 \leq \varepsilon$ and $(1-\varepsilon)v_2 \leq 1-\varepsilon$, it follows that

$$\varepsilon v_1 + (1-\varepsilon)v_2 \leq 1.$$

Hence,

$$0 \leq \varepsilon v_1 + (1-\varepsilon)v_2 \leq 1, \quad \forall v_1, v_2 \in U_{ad},\ \varepsilon \in [0,1].$$

A similar argument applies to the control w.

Therefore, U_{ad} is convex and Condition 2 is fulfilled.

Condition 3. Using the differential equations system (1), we consider the total population

$$N(t) = P(t) + H(t) + L(t).$$

Then, we get

$$\frac{dN}{dt} = \Omega - \mu N(t) \leq \Omega - \mu N(t).$$

So,

$$\lim_{t\to\infty} \sup N(t) \leq \frac{\Omega}{\mu}.$$

As a result, every solution for the controlled PHL model is bounded.

Hence, there exist positive constants R_1, R_2, and R_3 such that for all $t \in [t_0, t_f]$,

$$\begin{aligned} P(t) &\leq R_1, \\ H(t) &\leq R_2, \\ L(t) &\leq R_3. \end{aligned}$$

We then consider

$$\begin{cases} O_P = \dot{P}(t) \leq \Omega, \\ O_H = \dot{H}(t) \leq \dfrac{\alpha P(t)H(t)}{N} - w(t)H(t), \\ O_L = \dot{L}(t) \leq \beta P(t) + \gamma H(t) + v(t)R_1 + w(t)R_2. \end{cases}$$

Thus, the system can be rewritten in matrix form as

$$O(t; P, H, L) \leq \bar{A} + BX(t) - RU(t),$$

where

$$O(t; P, H, L) = \begin{bmatrix} O_P \\ O_H \\ O_L \end{bmatrix}, \quad \bar{A} = \begin{bmatrix} \Omega \\ 0 \\ 0 \end{bmatrix}, \quad X(t) = \begin{bmatrix} P \\ H \\ L \end{bmatrix}, \quad U(t) = \begin{bmatrix} v \\ w \end{bmatrix},$$

and

$$B = \begin{bmatrix} 0 & 0 & 0 \\ \frac{\alpha H}{N} & 0 & 0 \\ \beta & \gamma & 0 \end{bmatrix}, \quad R = \begin{bmatrix} 0 & 0 \\ 0 & H \\ -P & -H \end{bmatrix}.$$

The control vector and state variable vector are bounded by a linear function. Consequently, we can write

$$\|O(t; P, H, L)\| \leq \|\bar{A}\| + \|B\|\|X(t)\| + \|R\|\|U(t)\| \leq \psi + \Phi\left(\|X(t)\| + \|U(t)\|\right),$$

where $\psi = \|\bar{A}\|$ and $\Phi = \max(\|B\|, \|R\|)$.

Thus, the sum of the state and control vectors bounds the right-hand side. Consequently, Condition 3 is satisfied.

Condition 4. The integrand in the objective functional

$$J(v, w) = H(t_f) - L(t_f) + \int_{t_0}^{t_f} \left[H(t) - L(t) + \frac{M_1}{2}v^2(t) + \frac{M_2}{2}w^2(t)\right] dt$$

is convex on U_{ad}. The goal is to show that there exist constants $c_1, c_2 > 0$ and $\epsilon > 1$ such that the integrand

$$L(P, H, L, v, w) = H(t) - L(t) + \frac{M_1}{2}v^2(t) + \frac{M_2}{2}w^2(t)$$

satisfies

$$L(P, H, L, v, w) \geq -c_1 + c_2\big(|v|^2 + |w|^2\big)^{\epsilon/2}.$$

Since the state variables $P(t)$, $H(t)$, and $L(t)$ are bounded, we can take

$$\epsilon = 2, \quad c_1 = 2 \sup_{t \in [t_0, t_f]} (H(t), L(t)), \quad c_2 = \inf\left(\frac{M_1}{2}, \frac{M_2}{2}\right).$$

Consequently, it follows that

$$L(P, H, L, v, w) \geq -c_1 + c_2\left(|v|^2 + |w|^2\right).$$

Thus, the integrand of the objective functional is convex and Condition 4 is satisfied. □

In summary, by verifying all four conditions stated in the theorem namely, the non emptiness of the admissible set, the convexity and closedness of the control set, the linear boundedness of the system dynamics, and the convexity of the integrand, it is concluded that an optimal control pair

(v^*, w^*) exists for the controlled PHL model. This result ensures the mathematical soundness of the formulated optimal control problem and provides a rigorous foundation for the derivation of the necessary conditions for optimality, which will be explored in the subsequent subsection.

4.3 Characterization of optimal controls

In this part, we make use of Pontryagin's maximum principle [23]. The key idea is to use the adjoint function to produce the Hamiltonian function by connecting the differential equations system to the objective function. This idea transfers the problem of finding the control to optimize the objective functional subject to the system of differential equations with initial condition and then finds the control to optimize the Hamiltonian pointwise (concerning the control).
Using Pontryagin's maximum principle, the Hamiltonian function is defined as

$$\mathcal{H}(t) = H(t) - L(t) + \frac{M_1}{2}v^2 + \frac{M_2}{2}w^2 + \zeta_1 f_1 + \zeta_2 f_2 + \zeta_3 f_3,$$

where f_1, f_2, f_3 are the right-hand sides of the controlled state system.

Theorem 8. Given an optimal control $v^* = (v^*, w^*) \in U_{ad}^2$ and corresponding solutions P^*, H^*, and L^* of the state system (1), there exist adjoint functions ζ_1, ζ_2, and ζ_3 fulfilling

$$\begin{cases} \dot{\zeta}_1 = \zeta_1\Big\{\alpha\dfrac{H(t)}{N} + \beta + \mu + v(t)\Big\} - \zeta_2\alpha\dfrac{H(t)}{N} - \zeta_3\big\{\beta + v(t)\big\}, \\ \dot{\zeta}_2 = -1 + \zeta_1\alpha\dfrac{P(t)}{N} - \zeta_2\Big\{\alpha\dfrac{P(t)}{N} - \gamma - \mu - w(t)\Big\} - \zeta_3\big\{\gamma + w(t)\big\}, \\ \dot{\zeta}_3 = 1 + \zeta_3\mu \end{cases} \tag{8}$$

At the time t_f, the transversality conditions are given as follows:

$$\begin{aligned} \zeta_1(t_f) &= 0, \\ \zeta_2(t_f) &= 1, \\ \zeta_3(t_f) &= -1. \end{aligned}$$

Moreover, the optimal controls $v^*(t)$ and $w^*(t)$ for $t \in [t_0, t_f]$ are provided by

$$v^*(t) = \min\left\{1, \max\left\{0, \frac{1}{M_1}P(t)(\zeta_1(t) - \zeta_3(t))\right\}\right\}, \tag{9}$$

$$w^*(t) = \min\left\{1, \max\left\{0, \frac{1}{M_2}H(t)(\zeta_3(t) - \zeta_2(t))\right\}\right\}. \tag{10}$$

Proof. The Hamiltonian $\mathcal{H}$ at time t is defined by

$$\begin{aligned}\mathcal{H}(t) = H(t) - L(t) + \frac{M_1}{2}v^2(t) + \frac{M_2}{2}w^2(t)\\ +\zeta_1\Big\{\Omega - \alpha\frac{P(t)H(t)}{N} - (\beta+\mu)P(t) - v(t)P(t)\Big\}\\ +\zeta_2\Big\{\alpha\frac{P(t)H(t)}{N} - (\gamma+\mu)H(t) - w(t)H(t)\Big\}\\ +\zeta_3\Big\{\beta P(t) + \gamma H(t) - \mu L(t) + v(t)P(t) + w(t)H(t)\Big\}.\end{aligned}$$

Using Pontryagin's maximum principle, we obtain the transversality conditions and adjoint equations for $t \in [t_0, t_f]$ as follows:

$$\begin{aligned}\zeta_1(t_f) &= 0, & \dot{\zeta}_1(t) &= -\frac{\partial\mathcal{H}}{\partial P},\\ \zeta_2(t_f) &= 1, & \dot{\zeta}_2(t) &= -\frac{\partial\mathcal{H}}{\partial H},\\ \zeta_3(t_f) &= -1, & \dot{\zeta}_3(t) &= -\frac{\partial\mathcal{H}}{\partial L}.\end{aligned}$$

The optimality condition can be used to solve the optimal controls $v^*(t)$ and $w^*(t)$ for $t \in [t_0, t_f]$:

$$\frac{\partial\mathcal{H}}{\partial v} = M_1 v(t) + \zeta_1(t)(-P(t)) + \zeta_3(t)P(t) = 0,$$

$$\frac{\partial\mathcal{H}}{\partial w} = M_2 w(t) + \zeta_2(t)(-H(t)) + \zeta_3(t)H(t) = 0.$$

That is,

$$\begin{aligned}v(t) &= \frac{1}{M_1}P(t)(\zeta_1(t) - \zeta_3(t)),\\ w(t) &= \frac{1}{M_2}H(t)(\zeta_3(t) - \zeta_2(t)).\end{aligned}$$

It is straightforward to obtain $v^*(t)$ and $w^*(t)$ in the form of the optimal control laws derived previously, by applying the admissible bounds in U_{ad} for the controls.

Considering the bounds in U_{ad}, the optimal controls are projected as follows:

$$v^*(t) = \min\left\{1, \max\left\{0, \frac{1}{M_1}P(t)(\zeta_1(t) - \zeta_3(t))\right\}\right\},$$

$$w^*(t) = \min\left\{1, \max\left\{0, \frac{1}{M_2}H(t)(\zeta_3(t) - \zeta_2(t))\right\}\right\}.$$

□

In summary, the application of Pontryagin's maximum principle allows us to characterize the necessary conditions for optimal control of the digital platform dynamics. The resulting system, composed of the state equations, the adjoint system, and the optimality conditions, provides a complete framework for determining the optimal strategies $v^*(t)$ and $w^*(t)$. These controls respectively represent the most effective interventions for attracting potential customers and for converting hesitant users into loyal ones, while minimizing associated costs. The obtained results form the theoretical foundation for numerical simulations, which will further illustrate the impact of these optimal strategies on the overall engagement and loyalty within the digital platform ecosystem.

5 Numerical simulations

This subsection is dedicated to the numerical investigation of the controlled PHL model with the aim of evaluating the effectiveness of optimal intervention strategies in influencing customer behavior. Specifically, the model considers two types of customers: Hesitant customers (H), who are undecided about adopting the platform or service, and loyal customers (L), who consistently engage with the platform. By implementing two time-dependent control measures an incentive-based control $v(t)$ and a support-based control $w(t)$ we aim to reduce hesitation, increase loyalty, and optimize the overall performance of the platform within a given time horizon $[t_0, t_f]$.

The numerical simulations are performed using the forward-backward sweep method, which efficiently solves the coupled system of state and adjoint equations derived from Pontryagin's maximum principle. At each iteration, the state system is integrated forward in time using initial conditions, while the adjoint system is integrated backward from the terminal conditions. The controls are updated at each time step according to the optimality conditions, while ensuring that they remain within the admissible range $0 \leq v(t), w(t) \leq 1$. This iterative process continues until convergence is achieved, providing the optimal control trajectories (v^*, w^*) and the corresponding state dynamics. The convergence of this iterative scheme in a finite number of steps is guaranteed under the standard conditions established by Lenhart and Workman [17]: Specifically, when the time horizon T is sufficiently small relative to the Lipschitz constants of the state and adjoint systems, the forward–backward sweep contraction mapping argument ensures that the iterates

converge to the unique optimal solution. In our simulations, convergence is declared when the relative change in the control variables between successive iterations falls below a tolerance of 10^{-6}.

For the numerical simulations, the model parameters were selected based on realistic behavioral assumptions and calibrated to ensure meaningful system dynamics. The baseline parameter values were set as follows: $\Omega = 0.9$, $\alpha = 0.1$, $\beta = 0.4$, $\mu = 0.04$, and $\gamma = 0.01$, with a total population $N = 1400000$. These parameters respectively represent the recruitment rate of potential customers, the interaction rate between potential and hesitant individuals, the spontaneous transition rate toward adoption, the natural decay rate, and the reactivation rate of hesitant individuals. The simulation horizon was fixed at $T = 30$ time units, discretized into $M = 10{,}000$ steps to ensure numerical stability and accuracy.

The initial conditions were defined as $P(0) = 900{,}000$, $H(0) = 500{,}000$, and $L(0) = 0$, representing the initial distributions of potential, hesitant, and loyal customers, respectively. The adjoint variables were initialized with terminal conditions $\zeta_1(T) = 0$, $\zeta_2(T) = 1$, and $\zeta_3(T) = -1$, consistent with the transversality conditions of Pontryagin's maximum principle. The control parameters $M_1 = 60$ and $M_2 = 30$ were introduced as weighting factors in the cost functional, reflecting the relative cost of implementing promotional and awareness strategies. Using these settings, the model was simulated under both uncontrolled and controlled scenarios to analyze the temporal evolution of customer behavior and to evaluate the impact of optimal interventions on e-commerce adoption.

Through these simulations, several scenarios can be explored to understand the impact of control strategies on customer dynamics. For example, we can examine:

- Single-control strategies, where only the incentive-based control $v(t)$ or only the support-based control $w(t)$ is applied.
- Combined control strategies, where both $v(t)$ and $w(t)$ are optimally applied simultaneously.

Additionally, sensitivity analyses of key model parameters, such as the rates of transition between hesitant and loyal customers and the cost weights of the controls, are conducted to identify which factors most strongly influence customer retention and the effectiveness of interventions. These numerical experiments provide a comprehensive understanding of the dynamics of hesitant and loyal customers and offer practical insights into the design of efficient strategies for improving customer loyalty and engagement on digital platforms.

To investigate the evolution of potential, hesitant, and loyal customers and to assess the impact of time-dependent interventions, we implement a numerical scheme for the controlled

PHL model. The procedure involves forward integration of the state system using an explicit Euler method, backward integration of the adjoint system, and iterative updates of the control variables according to Pontryagin's maximum principle. This iterative process continues until convergence of both the state trajectories and control profiles is achieved. The complete numerical resolution algorithm is presented in Algorithm 1.

Algorithm 1 Numerical resolution scheme for the controlled PHL model

Input: Parameters $\Omega, \alpha, \beta, \gamma, \mu, M_1, M_2, N, T, M$
Initialize: $P(0), H(0), L(0)$; $\zeta_1(T), \zeta_2(T), \zeta_3(T)$; $v(0), w(0)$
Set time step $h = T/M$
repeat
  Forward integration (state system)
  for $i = 1$ to M **do**
    Compute derivatives:
    $\dot{P} = \Omega - \alpha P_i H_i/N - (\beta + \mu)P_i$
    $\dot{H} = \alpha P_i H_i/N - (\gamma + \mu)H_i$
    $\dot{L} = \beta P_i + \gamma H_i - \mu L_i$
    Update using Euler scheme:
    $P_{i+1} = P_i + h\dot{P}$
    $H_{i+1} = H_i + h\dot{H}$
    $L_{i+1} = L_i + h\dot{L}$
  end for
  Backward integration (adjoint system)
  for $i = M - 1$ down to 1 **do**
    Compute adjoint derivatives:
    $\dot{\zeta}_1 = \zeta_1(\alpha H_i/N + \beta + \mu + v_i) - \zeta_2(\alpha H_i/N) - \zeta_3(\beta + v_i)$
    $\dot{\zeta}_2 = -1 + \zeta_1(\alpha P_i/N) - \zeta_2(\alpha P_i/N - \gamma - \mu - w_i) - \zeta_3(\gamma + w_i)$
    $\dot{\zeta}_3 = 1 + \zeta_3\mu$
    Update adjoint variables:
    $\zeta_1(i) = \zeta_1(i+1) - h\dot{\zeta}_1$
    $\zeta_2(i) = \zeta_2(i+1) - h\dot{\zeta}_2$
    $\zeta_3(i) = \zeta_3(i+1) - h\dot{\zeta}_3$
  end for
  Update control variables:
  $v_{i+1} = \min(1, \max(0.5, (\zeta_1 - \zeta_3)P_{i+1}/M_1))$
  $w_{i+1} = \min(1, \max(0.5, (\zeta_3 - \zeta_2)H_{i+1}/M_2))$
until Convergence of P, H, L, v, w
Output: Time evolution of $P(t)$, $H(t)$, $L(t)$, $v(t)$, $w(t)$

Interpretation of the Evolution of Hesitant Customers $H(t)$

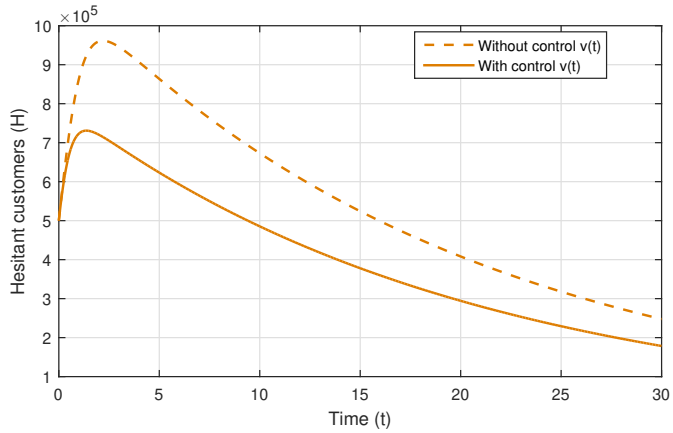

Figure 3: Dynamics of the hesitant model with control v

Figure 3 illustrates the temporal evolution of the hesitant customer population $H(t)$ with and without the implementation of the incentive-based control $v(t)$. In the absence of control, the number of hesitant customers exhibits a sharp and sustained increase, indicating the self-reinforcing nature of rumor propagation on digital platforms. This behavior reflects how misinformation can significantly amplify hesitation among potential users, leading to reduced platform trust and slower conversion to loyalty.

However, when the control $v(t)$ is applied, the curve demonstrates a pronounced decline in the hesitant population over time. This reduction underscores the effectiveness of incentive-driven strategies in mitigating the impact of rumor-induced hesitation. The control essentially acts as a stabilizing mechanism, accelerating the recovery of customer confidence by encouraging engagement and counteracting the deterrent effects of misinformation.

From a practical standpoint, this outcome highlights the role of proactive incentive policies such as reward systems, reputation mechanisms, or verified information campaigns in maintaining user trust. Mathematically, the control $v(t)$ modifies the transition rate from the hesitant to the loyal compartment, thereby reducing the effective reproduction number of hesitation dynamics. The overall effect is a faster convergence toward equilibrium and improved platform stability. In the uncontrolled case, $H(t)$ rises sharply from $H(0) = 500{,}000$, reaching a peak near $t \approx 8$ before declining gradually, a trajectory consistent with the endemic behavior predicted analytically when $\mathcal{R}_0 > 1$. Under control $v(t)$, the peak is both lower in magnitude and reached earlier, with $H(t)$ declining more steeply thereafter, confirming accelerated convergence toward the rumor-free equilibrium $\mathcal{E}_f$, consistent with the global stability result of Theorem 5.

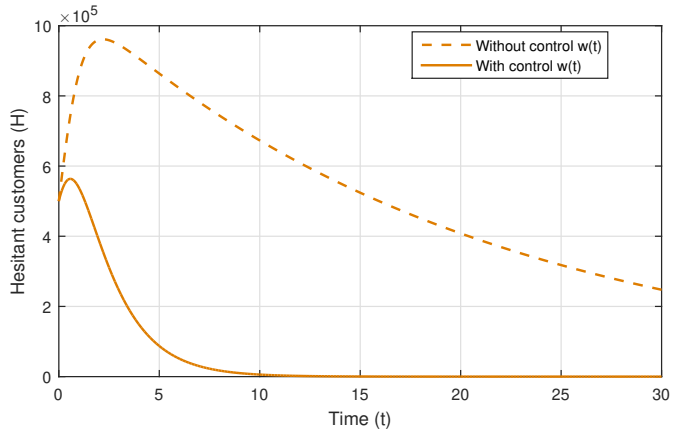

Figure 4: Dynamics of the hesitant model with control w

Figure 4 illustrates the temporal evolution of hesitant customers $H(t)$ under two scenarios: with and without the implementation of the support-based control $w(t)$. The control $w(t)$ represents platform-driven strategies such as user education campaigns, technical support, or trust-building initiatives designed to reduce uncertainty and hesitation among potential users.

In the absence of control, the number of hesitant customers initially rises sharply due to the unmitigated influence of rumor propagation and misinformation within the digital ecosystem. This increase reflects how hesitation naturally amplifies when corrective interventions are lacking, as negative perceptions spread faster among undecided users. Over time, the population of hesitant customers stabilizes at a relatively high level, indicating persistent behavioral stagnation and reduced user conversion toward loyalty.

Conversely, when the control $w(t)$ is applied, a noticeable decline in the hesitant customer population occurs after an initial transient phase. This reduction demonstrates the effectiveness of supportive interventions in mitigating rumor-driven hesitation and encouraging smoother transitions from the hesitant to the loyal customer compartment. The gap between the controlled and uncontrolled trajectories highlights the control's efficiency in fostering platform trust and engagement stability.

Overall, the results confirm that the support-based control $w(t)$ plays a crucial role in counteracting the spread of hesitation by reinforcing user confidence and limiting the long-term effects of misinformation. This finding underscores the importance of sustained and well-calibrated support initiatives in enhancing digital platform resilience and promoting sustained customer loyalty. Compared to the incentive-based control (Figure 3), the support-based control $w(t)$ achieves a faster and deeper suppression of hesitancy in the mid-range of the simulation, since $w(t)$ acts

directly on the H-compartment outflow rate, accelerating the conversion of hesitant users into loyal customers ($\gamma \to \gamma + w(t)$).

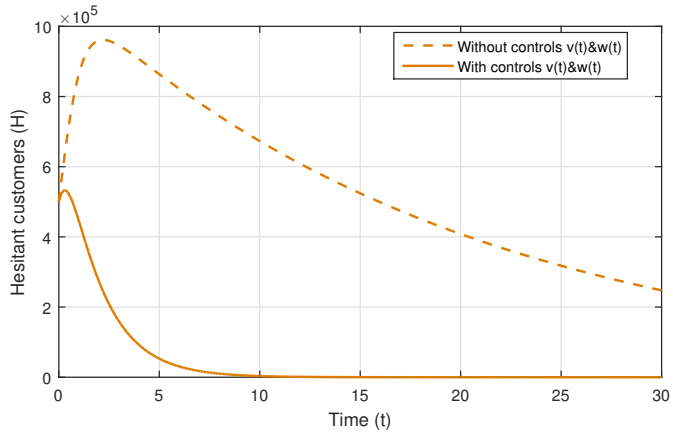

Figure 5: Dynamics of the hesitant model with controls v and w

Figure 5 illustrates the temporal evolution of hesitant customers when both incentive-based $v(t)$ and support-based $w(t)$ interventions are simultaneously implemented. From the plot, we observe that in the absence of controls, the hesitant population exhibits a sustained increase before stabilizing at a relatively high level, indicating that, without strategic intervention, rumor propagation continues to generate uncertainty and hesitation among potential customers. This behavior highlights the self-reinforcing nature of misinformation in digital ecosystems, once hesitation takes hold, it spreads through social influence and weakens customer confidence.

Conversely, under combined control strategies, the curve of hesitant customers declines significantly over time and stabilizes at a much lower equilibrium. This reduction demonstrates the effectiveness of deploying both interventions concurrently: The incentive-based control encourages user engagement and active participation, while the support-based control strengthens trust through guidance and educational measures. The synergy between these two controls accelerates the transition of hesitant users into loyal ones, mitigating the overall impact of rumor-induced hesitation.

Overall, this simulation confirms that multi-faceted intervention strategies outperform isolated approaches, reinforcing the importance of integrated policy design in managing rumor-driven behavioral dynamics. The results align with theoretical predictions from optimal control analysis, validating that the joint optimization of economic incentives and informational support effectively stabilizes customer behavior in the digital environment. This synergistic effect arises because $v(t)$ reduces the inflow of new hesitant users (by converting potential customers directly

to loyalty), while $w(t)$ accelerates the outflow of existing hesitant users toward loyalty, together driving $H(t)$ to near-zero levels by approximately $t \approx 10$, as predicted by Theorems 7 and 8.

Remark 3. The three simulations collectively demonstrate that both incentive-based (v(t)) and support-based (w(t)) controls effectively reduce the number of hesitant customers compared to the uncontrolled case. While each control independently mitigates hesitation, their combined application yields the most significant improvement, accelerating customer transition toward loyalty. This confirms that integrating motivational and informational interventions enhances overall platform stability and resilience against rumor-induced hesitation.

Interpretation of the Evolution of Loyal Customers $L(t)$

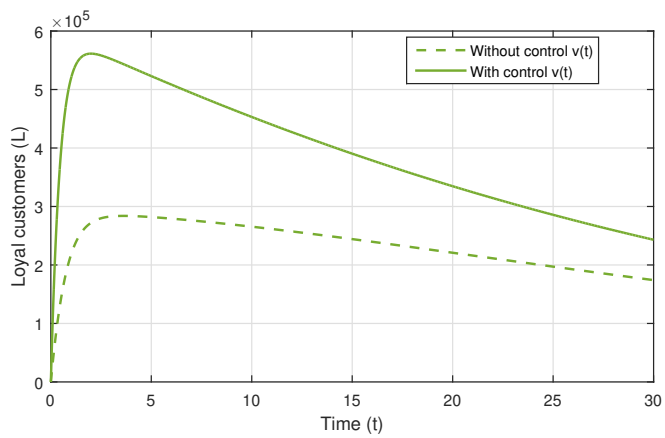

Figure 6: Dynamics of the loyal model with control v

Figure 6 illustrates the temporal evolution of the loyal customer population $L(t)$ under two scenarios: With and without the incentive-based control $v(t)$. In the absence of control, the number of loyal customers exhibits a slow and modest increase, stabilizing around approximately 30,000 individuals by the end of the simulation period. This limited growth reflects the natural rate of customer transition toward loyalty when no proactive interventions are applied, leaving the system more vulnerable to rumor-driven hesitation.

In contrast, when the control $v(t)$ is implemented, the curve shows a rapid and substantial rise in loyalty, reaching nearly 85,000 loyal customers over the same time horizon. This pronounced improvement highlights the effectiveness of incentive mechanisms such as promotional campaigns, loyalty rewards, or positive information reinforcement in converting hesitant users into committed customers. Moreover, the controlled trajectory remains stable throughout, indicating that the strategy effectively mitigates the destabilizing effects of rumor dissemination.

Overall, these numerical outcomes demonstrate that the application of $v(t)$ not only enhances customer retention but also fortifies the system's resilience against misinformation, ensuring a more robust and trustworthy digital platform ecosystem.

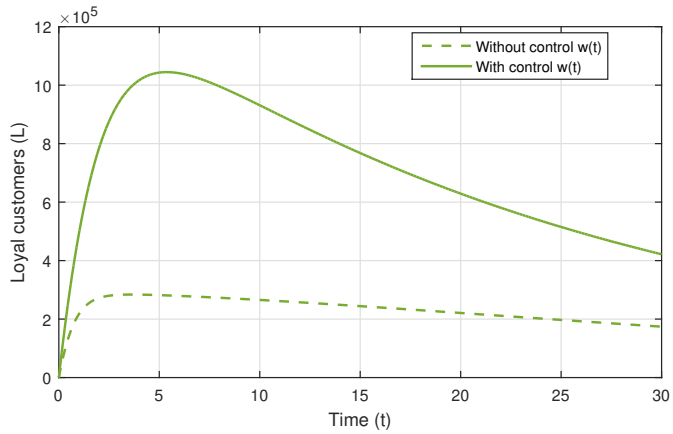

Figure 7: Dynamics of the loyal model with control w

The results illustrated in Figure 7 compare the evolution of loyal customers $L(t)$ under two scenarios: With and without the implementation of the control $w(t)$. Without control, the loyal customer population remains relatively stagnant, stabilizing near 6.0×10^5 by the end of the simulation period. In contrast, when the control is activated, $L(t)$ exhibits a marked increase, reaching approximately 1.2×10^6 after 30 time units, almost a twofold improvement.

This outcome underscores the crucial role of $w(t)$ in mitigating the negative influence of rumor propagation on user confidence and loyalty. By reducing rumor-induced hesitation, the control promotes a faster and more sustained transition of users toward loyalty. The observed acceleration in loyalty growth highlights the efficiency of targeted rumor refutation and trust reinforcement interventions, confirming the effectiveness of the proposed strategy in enhancing both user engagement and platform stability. The improvement is sustained and monotone from the early stages of the simulation, reflecting the direct impact of $w(t)$ on the $H \to L$ transition rate, and has direct practical relevance for platform managers: Investment in user support infrastructure (e.g., FAQ systems, live assistance, trust verification badges) produces long-run loyalty gains that outweigh short-term implementation costs.

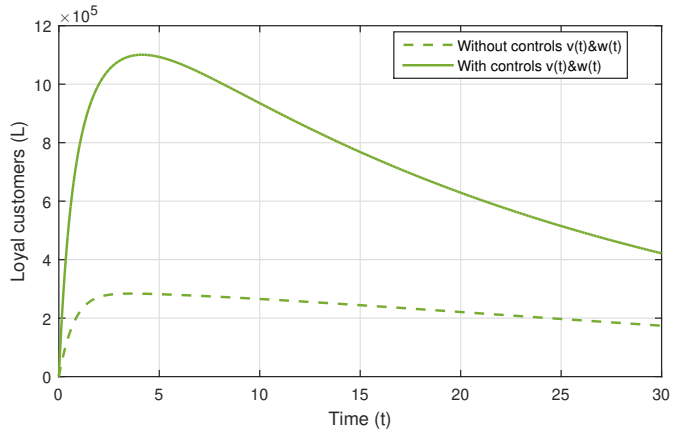

Figure 8: Dynamics of the loyal model with controls v and w

The simulation depicted in Figure 8 illustrates the temporal evolution of loyal customers $L(t)$ under both controlled and uncontrolled scenarios involving the two strategies $v(t)$ and $w(t)$. Initially, the population of loyal users increases gradually. However, in the absence of controls, the curve stabilizes at a significantly lower level around 6×10^5, reflecting the persistent impact of rumor propagation, which erodes trust and discourages long-term engagement.

When both control strategies are simultaneously applied, the growth of loyal customers accelerates markedly, reaching nearly 1.2×10^6 by the end of the simulation period ($t = 30$). This represents an approximate doubling in loyalty rates compared to the uncontrolled case. The combined influence of $v(t)$ (incentive-based) and $w(t)$ (support-based) interventions effectively counteracts the hesitation induced by rumors, restoring confidence and fostering retention.

Overall, the figure underscores the synergistic effect of applying integrated control mechanisms: While rumor dynamics naturally hinder user loyalty, coordinated actions to both incentivize potential users and reinforce hesitant ones can significantly mitigate misinformation's adverse impact, leading to a more resilient and trustworthy digital system.

Remark 4. The comparative analysis of the three figures highlights the effectiveness of the proposed control strategies in mitigating rumor-induced hesitation and enhancing customer loyalty. While uncontrolled dynamics reveal the detrimental influence of rumor dissemination on customer engagement, the implementation of the incentive based control $v(t)$ and the support based control $w(t)$, especially when applied jointly demonstrates a substantial improvement in stabilizing hesitant users and promoting loyalty. These findings confirm that coordinated interventions not only suppress the negative behavioral impact of rumors but also foster sustainable platform growth.

6 Conclusion

This study proposed and analyzed an optimal control model that captures the rumor-induced behavioral dynamics of customers on digital platforms. Drawing inspiration from epidemiological modeling, the developed PHL framework divides the customer population into potential, hesitant, and loyal compartments, with transitions driven by the diffusion of rumors. The model formalizes how misinformation can propagate through user interactions, fostering hesitation and reducing loyalty, while also providing a means to assess and mitigate these effects through optimal control strategies. The incorporation of incentive-based and support-based control functions enables the design of interventions that not only suppress the negative impact of rumors but also encourage customer engagement and trust restoration. Theoretical analysis, supported by Pontryagin's maximum principle, established the existence and characterization of optimal controls, offering a systematic foundation for decision-making. Sensitivity analysis of the basic reproduction number (R_0) revealed the dominant parameters influencing rumor persistence, highlighting which behavioral or informational levers are most effective in minimizing the spread of hesitation. Numerical simulations conducted using a forward–backward sweep method based on an explicit Euler discretization scheme demonstrated the practical implications of these findings. The results showed that the combined application of incentive and support controls markedly reduces the hesitant population, curtails rumor propagation, and accelerates the growth of loyal users, thereby reinforcing platform stability and credibility. In summary, this research bridges rumor dynamics, behavioral modeling, and optimal control theory into a unified mathematical approach for digital ecosystems. It provides both analytical depth and strategic insight into how misinformation can be contained and counteracted. Future studies may extend this model to stochastic or network-based settings, integrate real-time data, or explore adaptive rumor countermeasures, further enhancing the applicability of mathematical control frameworks in addressing the societal and economic challenges posed by digital misinformation.

Funding

This research received no external funding.

Conflicts of Interest

The authors declare no conflicts of interest.

References

[1] Amini, A., Bayiz, Y.E., Lee, E.-J., Somer-Topcu, Z., Mărculescu, R. and Topcu, U. *How media competition fuels the spread of misinformation*, Sci. Adv. 11(25) (2025), eadu7743..

[2] Baek, J., Dinev, A. and Lykouris, T. *Social learning with bounded rationality: Negative reviews persist under newest first*, In Proceedings of the 25th ACM Conference on Economics and Computation (pp. 375–375) 2024.

[3] Bakenova, K., Kuznetsov, A., Artyshchuk, I., Shaikhanova, A., Shevchuk, R. and Orobchuk, O. *Information diffusion modeling in social networks: A comparative analysis of delay mechanisms using population dynamics*, Appl. Sci. 15(11) (2025), 6092.

[4] Belhdid, S., Balatif, O. and Khajji, B. *Optimal control and cost-effectiveness analysis of scam rumor propagation over social networks*, Results Control Optim. 16 (2024), 100441.

[5] Boyce, W.E. and DiPrima, R.C. *Elementary differential equations and boundary value problems*, John Wiley and Sons, New York, 2009.

[6] Chen, J., Zhang, L. and Wang, X. *SEIOR rumor propagation model considering hesitating mechanism*, Mathematics 11(2) (2023), 283.

[7] Danenberg, T. and Fudenberg, D. *Endogenous attention and the spread of false news*, arXiv:2406.11024 (2024).

[8] Ding, J., Li, Z., Wu, X., Liu, R. and Hu, H. *Information dissemination model based on social networks characteristics*, Mathematics 13(8) (2025), 1254.

[9] El Bhih, A., Yaagoub, Z., Rachik, M. and Allali, K. *Controlling the dissemination of rumors and antirumors in social networks: A mathematical modeling and analysis approach*, Eur. Phys. J. Plus 139(2) (2024), 1–23.

[10] Fleming, W.H. and Rishel, R.W. *Deterministic and stochastic optimal control*, Springer, New York, 1975.

[11] Gonen, L.D., Tavor, T. and Spiegel, U. *Unlocking market potential: Strategic consumer segmentation and dynamic pricing for balancing loyalty and deal seeking*, Mathematics 12(21) (2024), 3364.

[12] Iranmanesh, A. and Rahgozar, M. *IMEGAR: An enhanced hybrid genetic algorithm for dynamic influence maximization in social networks*, Research Square (2024).

[13] Jakobsen, L., Holden, A.J., Gürcan, Ö. and Özgöbek, Ö. *Agent-based exploration of recommendation systems in misinformation propagation*, In Social Simulation Conference, pp. 269-284. Cham: Springer Nature Switzerland, 2025.

[14] Kang, S., Hou, X., Hu, Y. and Liu, H. *Dynamic analysis and optimal control considering cross transmission and variation of information*, Sci. Rep. 12(1) (2022), 17245.

[15] Laaroussi, A.E.A., El Bhih, A. and Rachik, M. *Optimal vaccination and treatment policies with constrained inequalities to study limited vaccination resources for a multistrain reaction-diffusion SEIR model of COVID-19*, Partial Differ. Equ. Appl. Math. 10 (2024), 100684.

[16] LaSalle, J.P. *The stability of dynamical systems*, Regional Conference Series in Applied Mathematics, Vol. 25, SIAM, Philadelphia, 1976.

[17] Lenhart, S. and Workman, J.T. *Optimal control applied to biological models*, Chapman & Hall/CRC, Boca Raton, 2007.

[18] Li, D., Zhao, Y. and Deng, Y. *Rumor spreading model with a focus on educational impact and optimal control*, Nonlinear Dyn. 112(2) (2023), 1575–1592.

[19] Li, S. and Zhang, Q. *Dynamics analysis and optimal control of rumor propagation in online platforms*, Comput. Math. Methods Med. (2025), 5503137.

[20] Liu, F., Zhang, Z. and Buss, M. *Robust optimal control of deterministic information epidemics with noisy transition rates*, Physica A 517 (2018), 577–589.

[21] López, A.B., Pastor-Galindo, J. and Ruipérez-Valiente, J.A. *Frameworks, modeling and simulations of misinformation and disinformation: A systematic literature review*, arXiv:2406.09343 (2024).

[22] Mansal, F. and Faye, I. *Mathematical modeling and optimal control of untrue information: Dynamic SEIZ in online social networks*, arXiv:2309.13058 (2023).

[23] Pontryagin, L.S., Boltyanskii, V.G., Gamkrelidze, R.V. and Mishchenko, E.F. *The mathematical theory of optimal processes*, Wiley, New York, 1962.

[24] Van den Driessche, P. and Watmough, J. *Reproduction numbers and subthreshold endemic equilibria for compartmental models of disease transmission*, Math. Biosci. 180(1–2) (2002), 29–48.

[25] Wu, H. and Li, J. *Analysis and control of rumor propagation model with repeated waiting behavior*, Mathematics 13(2) (2025), 312.

[26] Yaagoub, Z., El Bhih, A. and Allali, K. *Global analysis of a fractional-order infection model for the propagation of computer viruses*, Model. Earth Syst. Environ. 11(1) (2025), 68.

[27] Zheng, W. and Liu, Y. *Research on rumor and anti-rumor propagation models in social networks*, Sci. Rep. 15 (2025), 96006.